Journal of Theoretical and Applied Mechanics, Sofia, 2003, vol. 33, No. 2, pp. 29-40

FLUID MECHANICS

NUMERICAL VERIFICATION OF THE CASSIE'S EQUATION FOR WELL-DEFINED HETEROGENEOUS SUBSTRATES WITH "MESA" DEFECTS

N. Pesheva, S. Iliev

Institute of Mechanics, Bulgarian Academy of Sciences,
Acad. G. Bonchev Str. Bl. 4, 1113 Sofia, Bulgaria,
e-mails: nina@imbm.bas.bg, stani@imbm.bas.bg

[Received 13 December 2002. Accepted 17 March 2003]

Abstract. The wetting properties of model heterogeneous flat substrates are studied numerically. In the framework of the classical capillary theory the shapes of three-dimensional liquid drops in equilibrium with such substrates are obtained. The numerical method used is based on the local variations approach. It has been extended here to treat chemically heterogeneous substrates with "mesa" defects, i.e. sharp boundaries between surface patches with different surface tensions. We discuss the implications for the Cassie's equation.
Key words: Cassie's law, contact angles, heterogeneous substrates, liquid drops.

1. Introduction

Contact angles carry important information about the surfaces and measurements of the contact angles are among the most used ways of characterising the surfaces in scientific and industrial laboratories. The chemical heterogeneity and/or roughness can cause serious technical problems in determining the contact angles and in general the problem is unsolvable by analytical approaches only. Theoretical analysis is extremely difficult for such surfaces. Thus numerical methods and computer simulations have proved very useful and have gained significant importance supplementing the theoretical and experimental studies.

We report here our preliminary results on the wetting properties of well defined heterogeneous surfaces. More detailed study is under way. In this work we obtain and analyse the numerical solutions for drop shapes and contact angles within the framework of the classical capillary theory on smooth but chemically heterogeneous model surface with well defined structure. The considered model solid surface consists of two types of homogeneous patches,

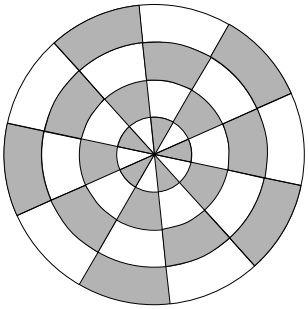

Fig. 1. Model surface substrate consisting of radial sectors crossed with concentric circles with check-mate patches of different surface tensions (dart-board substrate)

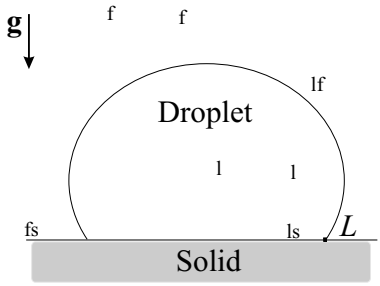

Fig. 2. Schematic drawing of the three phase system consisting of a liquid drop placed on a solid surface in ambient fluid

as illustrated in Fig. 1, that of radial sectors crossed with concentric circles with check-mate patches of different surface tensions (dart board substrate). These surfaces are quite similar to the ones used for theoretical discussion in [1] and also to the experimental substrates in [2]. To the best of our knowledge in such a general case numerical solutions are not available up to now.

For such two-component surfaces Cassie [3] proposed a semiempirical equation (widely known in the literature as Cassie's law) describing the averaged cosine of an effective contact angle θ^C through the cosines of the contact angles $\theta^{(1)}$, $\theta^{(2)}$ on the pure substrates with weights, given by the corresponding fractional areas f_1, f_2, of the two types of surfaces:

$$\cos\theta^C = f_1 \cos\theta^{(1)} + f_2 \cos\theta^{(2)}. \tag{1.1}$$

The cosines of the intrinsic contact angles that the drop would take on the pure substrates are expressed in terms of the corresponding interfacial energies through the well known Young equation:

$$\sigma_{lf} cos\theta^{(1)} = \sigma_{sf}^{(1)} - \sigma_{sl}^{(1)}, \quad \sigma_{lf} cos\theta^{(2)} = \sigma_{sf}^{(2)} - \sigma_{sl}^{(2)}. \tag{1.2}$$

$\sigma_{sl}^{(i)}$, $\sigma_{sf}^{(i)}$ and σ_{lf} are the interfacial energies; l, f and s subscripts refer to the liquid, fluid and solid respectively; the superscript $i = 1, 2$ refer to the two types of surfaces with different chemical properties (see Fig. 2).

A number of experimental studies found good agreement of the Cassie equation with the measured apparent contact angle, see e.g. [3–5]. Other

studies though report deviations from the Cassie equation [1, 2, 6]. Theoretical studies of the effect of inhomogeneity of the substrate on the contact line and on the contact angle of a drop are based on [7]. Two types of heterogeneities are considered – regular and "mesa" defects (i.e. sharp boundaries between patches with different surface tensions). In the case of "mesa" type heterogeneities the final shape of the liquid drop depends not only on the surface energies but also on the details of the patch structure of the surfaces and also on the manner in which the liquid drop is placed on the solid surface. All the above features give their reflection on the Cassie equation and the possibilities for different interpretations. The averaged cosine of the contact angle could be obtained by averaging over all possible equilibrium states at a given point of the substrate [8], it could be averaged along the contact line of a single drop and then over all possible contact lines [8], over subset of the possible contact lines [9] (since some of the contact lines could not be observed experimentally), only along the equilibrium state with the (absolute) minimal energy [10]. Moreover, quite often in the experiments instead of the contact angle its projection is measured and this has to be taken into account when analysing the Cassie's equation on heterogeneous substrates. Dynamic studies of spreading on heterogeneous substrates are undertaken by molecular dynamics simulations [11], simulation of Ising models [12], Monte Carlo simulations of solid-on-solid models [13], and Monte Carlo simulations of macroscopic Hamiltonian [14]. The simulation results in [11,12] show good agreement with theory, i.e. with Cassie's prediction. Numerical solutions for the shape of a drop on heterogeneous substrates were obtained in [15] by minimisation of the free energy of the capillary theory. The case of smoothly changing surface tension was considered there and the gravity is not taken into account.

This work is organised as follows. In the next section the model is formulated. We derive a condition for the contact angle when the contact line crosses or pins to the border between patches with different surface tensions with sharp boundaries. In Section 3 a short description is given of the numerical procedure. It is similar to the one used in the public domain software "Evolver" [16]. In the next Section 4 we obtain and discuss the numerical solutions (i.e. the local minima of the free energy) for drop shapes and contact angles within the framework of the classical capillary theory, taking into account the gravity. We discuss the implications of these solutions and the way the averaging of the contact angles is performed for the Cassie equation. In the last section the results are summarised.

2. The model

We consider a 3D liquid drop placed on a horizontal, smooth and chemically heterogeneous solid surface. Both the drop and the substrate on which

it is placed are immersed in an ambient fluid and it is assumed that the liquid and fluid are mutually immiscible (see Fig. 2). Taking into account the gravity and considering the position-dependent interfacial energies σ_{lf}, σ_{sf} and σ_{sl}, the free energy of the system F which needs to be minimised with respect to the fluid-liquid interface in order to determine the equilibrium states is:

$$F = \int\limits_{\Sigma_{lf}} \sigma_{lf} d\Sigma_{lf} + \int\limits_{\Sigma_{ls}} \sigma_{ls} d\Sigma_{ls} + \int\limits_{\Sigma_{fs}} \sigma_{fs} d\Sigma_{fs} + \int\limits_{\Omega_l} \rho_l U_{gr} d\Omega_l + \int\limits_{\Omega_f} \rho_f U_{gr} d\Omega_f. \tag{2.1}$$

The subscripts l refers to the liquid; f to the ambient fluid; s to the solid surface; lf, ls and fs refer to the surfaces Σ (with the corresponding surface tension σ) between liquid/fluid, liquid/solid, and fluid/solid, respectively. The volume and the density of the droplet and the ambient fluid are denoted by Ω_l, ρ_l and Ω_f, ρ_f correspondingly. U_{gr} is the potential of the gravitation field $\mathbf{g}$ ($\mathbf{g} = -\mathrm{grad}\, U_{gr}$). The considered model substrate, shown in Fig. 1, in cylindrical co-ordinate system (r, φ, z) can be written as sets of two types of patches, with constant surface energies $\sigma_{ls}^{(1)}$, $\sigma_{fs}^{(1)}$ and $\sigma_{ls}^{(2)}$, $\sigma_{fs}^{(2)}$:

$$\Sigma_s = \left\{ \Sigma_{ij} = r, \varphi \;\middle\|\; \frac{2(i-1)\pi}{N_{sect}} \le \varphi < \frac{2i\pi}{N_{sect}},\ je \le r < (j+1)e; \right.$$
$$\left. i = 1, \ldots, N_{sect},\ j = 0, 1, 2, \ldots, N_r \right\}. \tag{2.2}$$

Here N_{sect} and N_r, e are parameters characterising the partitions along the polar angle φ and the radius r respectively.

We introduce the following set of independent variables:

$$b = (\rho_l - \rho_f) g/\sigma_{lf},\ \cos\theta^{(1)} = (\sigma_{ls}^{(1)} - \sigma_{fs}^{(1)})/\sigma_{lf},\ \cos\theta^{(2)} = (\sigma_{ls}^{(2)} - \sigma_{fs}^{(2)})/\sigma_{lf}. \tag{2.3}$$

To find the local minima of the free energy we first change the variables to the dimensionless variables $X = x/a$, $Y = y/a$, $Z = z/a$, where $a = 1/\sqrt{b}$ is the capillary length. Minimisation of the following dimensionless expression for the free energy while constraining the drops' volume to a fixed value, yields the equilibrium form of the drop:

$$F = -\cos\theta^{(1)} \int\limits_{\Sigma_{ls}^{(1)}} d\Sigma_{ls}^{(1)} - \cos\theta^{(2)} \int\limits_{\Sigma_{ls}^{(2)}} d\Sigma_{ls}^{(2)} + \int\limits_{\Sigma_{lf}} d\Sigma_{lf} + \int\limits_{\Omega_l} z d\Omega_l. \tag{2.4}$$

Special attention has to be paid to the equilibrium condition for the contact angle in the case of "mesa" defects. The standard condition at any

point $\mathbf{r}$ of the contact line L, for mechanical equilibrium $\delta F = 0$ with respect to any shift $\delta\mathbf{r}$ of the line position leads to the classical Young equation (1.2) for the contact angle θ for every homogeneous patch with surface tension $\sigma_{ls}^{(i)}$, $i = 1, 2$. However, when the point $\mathbf{r}$ of the contact line belongs to the border between two patches with different surface tensions $\sigma_{sl}^{(1)}$ and $\sigma_{sl}^{(2)}$ respectively, then the virtual work done for a virtual shift $\delta\mathbf{r}$ of the contact line depends on the position of the point $\mathbf{r} + \delta\mathbf{r}$. That is, if $\mathbf{r} + \delta\mathbf{r}$ belongs to the substrate with $\sigma_{sl}^{(1)}$, then the virtual work done for this shift is:

$$\sigma_{lf}\left[\cos\theta - \cos\theta^{(1)}\right]\ \mathbf{e}\cdot\delta\mathbf{r}, \tag{2.5}$$

where $\mathbf{e}$ is the unit vector normal to the contact line L and tangent to the liquid-solid interface and is pointing outward the liquid-solid interface. Then the point $\mathbf{r} - \delta\mathbf{r}$ belongs to the substrate with $\sigma_{sl}^{(2)}$ and the virtual work done for this shift is:

$$-\sigma_{lf}\left[\cos\theta - \cos\theta^{(2)}\right]\ \mathbf{e}\cdot\delta\mathbf{r}. \tag{2.6}$$

Thus the condition for equilibrium leads to the requirement the following two conditions to be satisfied simultaneously:

$$\left[\cos\theta - \cos\theta^{(1)}\right](\delta\mathbf{r}\cdot\mathbf{e}) \le 0, \tag{2.7}$$

$$-\left[\cos\theta - \cos\theta^{(2)}\right](\delta\mathbf{r}\cdot\mathbf{e}) \le 0 \tag{2.8}$$

Having this in mind and taking into account the direction of the principal normal of the contact line, one arrives to the following condition for the equilibrium contact angle:

$$\cos\theta^{(2)} \le \cos\theta \le \cos\theta^{(1)}, \tag{2.9}$$

when the extrinsic normal $\mathbf{e}$ is pointing inwards the type (1)- parts or:

$$\cos\theta^{(1)} \le \cos\theta \le \cos\theta^{(2)}, \tag{2.10}$$

when the extrinsic normal $\mathbf{e}$ is pointing inwards the type (2)-parts. It has to be noted, that for every specific choice of the parameters $(\cos\theta^{(1)}, \cos\theta^{(2)})$ only one of the two conditions (2.9) and (2.10) holds. The obtained condition is similar to the condition for equilibrium on an edge [17].

One can expect nontrivial results for the averaged contact angle when along significant parts of the drop contact line the contact angle satisfies the condition (2.9) or (2.10). Then significant deviations from the Cassie's equation could be expected.

One way to find the averaged cosine of the contact angle for a given equilibrium drop shape [8] is to average along the contact line:

$$\cos\theta^{(a)} = \frac{\int\limits_L \cos\theta\,(L)\,dL}{\int\limits_L dL}. \tag{2.11}$$

In some cases it is difficult to determine experimentally the length of the contact line, then averaging along the polar angle φ can be used instead:

$$\cos\theta^{(b)} = \frac{1}{2\pi}\int\limits_0^{2\pi} \cos\theta\,(\varphi)\,d\varphi. \tag{2.12}$$

In some experiments the contact angle of a drop is determined by the projection of the drop on a given plain, e.g. in [18] the apparent (or else the observable) contact angle on heterogeneous surfaces is defined as the angle measured between the tangent to the surface of the solid at given point of the contact line and the tangent to the liquid-fluid interface at the same point. It is not a priori clear whether the apparent contact angle equals the intrinsic one. Then in the averaging (2.11) or (2.12) instead of the intrinsic contact angle (1.2), one should use the "projection contact angle".

3. Solution technique

Here, only a very concise description will be given of the numerical procedure. The interested reader is referred for more details to [19], where the method was developed and used for homogeneous substrates. In the present work the method was extended for chemically inhomogeneous substrates (2.2) to take into account the change in the energy of the drop base when the shape of the drop is changed.

The equilibrium drop shapes were calculated by minimising the system free energy – eq. (2.4) under the constant volume constraint. The numerical method is essentially an iterative minimisation procedure based on the local variations method [20]. The drop shape is approximated by a triangulation using N points. The free energy (2.4) is expressed in terms of the co-ordinates of the N points. The change of the drop shape is achieved by approximation of the virtual displacements. In the $3N$-co-ordinate space, the set of all possible

displacements of the N points is considered while keeping the volume constant and taking into account other constraints. In this work we use total of $N = 2971$ points for the drop shape, where the contact line is approximated by 180 points (see Fig. 4). We use Monte Carlo scheme for choosing the points which we will try to move. At every step the drop shape is changed in such way so that the free energy is decreased while the drop volume is kept constant. Thus eventually a local minimum is reached. The obtained equilibrium state depends, if it is not unique, on the initial state, from which the minimisation was started. In the algorithm used there are no explicit conditions for the contact angles of the drop. The values of the contact angles are determined as a result of the minimisation process (i.e. the obtained shape of the drop) and the surface energies for the substrates used. The contact angle at every point of the approximation of the contact line is determined after the minimisation process has stopped. It is defined as the angle between the plane of the substrate and the plane of the approximating triangle whose corner coincides with that point. The accuracy of the numerical procedure is very high; it allows to determine the contact angle with an error of the order of 1° as compared to the theoretical intrinsic contact angle given by the Young equation (1.2).

4. Results and discussion

We study two-component substrates with surface tensions $\sigma_{ls}^{(i)}$, $i = 1, 2$ for which the Young equation gives $\theta^{(1)} = 40^\circ$, $\theta^{(2)} = 90^\circ$, with surface fractions $f_1 = f_2 = 0.5$. The equilibrium drop shapes are obtained for the following set of parameters: $b = 1$, $V = 0.475$, (see (2.3)). We consider here only the case when $N_{sect} = 10$, $N_r = 60$, $e = 0.039$ (see (2.2)), which incorporates all important features concerning the Cassie equation and the interpretation of the experimental data. These parameters are close to the parameters of the system studied experimentally in [1,2] – that of a water drop with base diameter of 2-3 mm. The theoretical value, calculated according to the Cassie equation (1.1), for the so chosen parameters, is $\theta^C = 67.5^\circ$

When the minimisation procedure starts from axially symmetric drop shapes (centred at $r = 0$) with initial contact angle $\theta^0 = \text{const} \in [20^\circ, 110^\circ]$, we get nine different equilibrium solutions. The initial drop shapes are solutions to the Laplace equation with $b = 1$, $V = 0.475$ and fixed contact angle. In principle, the number of different possible solutions depends on N_{sect} and N_r. The nine solutions are obtained by starting the minimisation procedure from equilibrium drop shapes (in equilibrium with homogeneous substrates) whose radii lie between two successive concentric circles. These solutions are enumerated in Table 1. We have assumed that in this virtual experiment one can control how and where the drop is deposited on the surface. Other solutions are also possible when the initial drop shape is not axially symmetric, or is not

centred but we do not consider them.

Table 1. The values of the effective contact angles corresponding to the nine solutions

θ^0	(1) 90°	(2) 83°	(3) 75°	(4) 67°	(5) 60°	(6) 54°	(7) 50°	(8) 44°	(9) 40°
$\theta^{(a)}$	86.12°	80.66°	74.03°	67.31°	60.91°	54.99°	49.64°	44.86°	41.29°
$\theta^{(b)}$	86.13°	80.87°	74.38°	67.66°	60.98°	55.26°	49.9°	45.0°	41.32°
$\theta^{(b)}_{proj}$	84.75°	72.86°	63.5°	57.54°	52.96°	48.37°	44.77°	41.87°	40.56°

Some of the possible equilibrium contact lines are shown in Fig. 3. The inner (solution (1)) and the outer (solution (9)) contact lines consist of two alternating parts, one coinciding with the bordering concentric circle, and the other part lies entirely in the corresponding homogeneous sector. The rest of the contact lines consist of parts coinciding with the borders between different patches (i.e. with sections of the inner or outer concentric circles between which lies the contact line of the initial drop). The final 3D equilibrium drop shape is shown for solution (5) in Fig. 4.

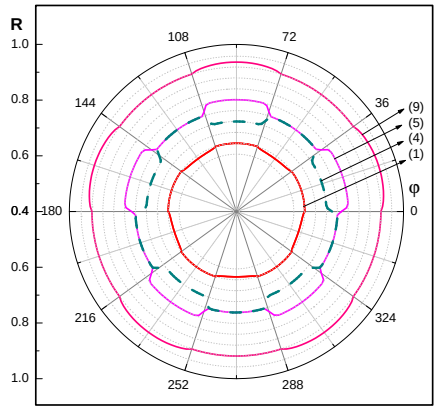

Fig. 3. The contact lines (the solid and dashed lines) for several solutions ((1), (4), (5) and (9) in Table 1) are shown. The dotted lines are the concentric circles serving as borders between the patches with different surface tensions

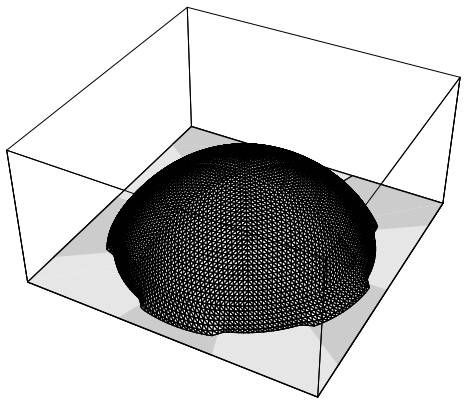

Fig. 4. The final 3D equilibrium drop shape is shown for solution (5) in Table 1

The contact angle, corresponding to the contact line of solution (5) in Fig. 3, is shown in polar co-ordinates in Fig. 5 with the solid line. The

dashed line in the same figure is the "projection contact angle" when the drop shape is projected onto the surfaces $\{\varphi = 2i^\circ\}$, $i = 0, \ldots, 180$. The difference between the solid line and the dashed line shows what will be the difference between the measured (or the observable contact angle) and the real contact angle for this substrate and the obtained shape. This could be the origin of the discrepancy between the experimental data with the theoretical predictions in some experimental studies.

As can be seen from Fig. 5, on the parts of the contact line coinciding with parts of the bordering concentric circles, the angles do not satisfy the Young equation but the condition (2.9). On the first and the last contact lines, approximately on the half of the contact lines the Young equation holds and on the other half (2.9) holds. It has to be stressed that on the parts of the contact line sticking to the concentric circles, the contact angle is not constant. The specific values of the contact angle (in the interval given by (2.9)) depends on the position of the point on the contact line with respect to the system of homogeneous patches and the distance from the centre of the drop (axis of symmetry).

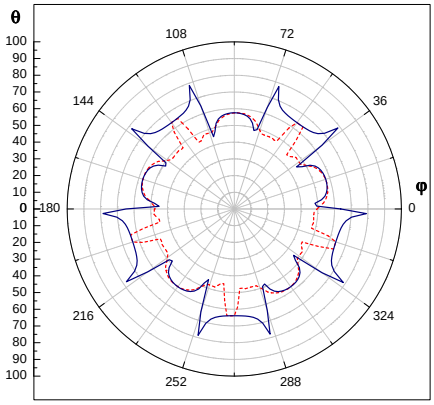

Fig. 5. The contact angle (solid line) and the projection contact angle (dashed line) as functions of the polar angle φ are shown for solution (5) in Table 1

The effective contact angles corresponding to the averaged cosines of the contact angles when the averaging is performed according to (2.11) and to (2.12) are given in Table 1. Also the averaged "projection contact angle" is given averaged according to (2.12) for all possible (nine in this particular example) centred equilibrium solutions starting with the one with the smallest

radius. In the first row of Table 1 exemplary values of the initial contact angles are given of the initial drop shapes on homogeneous substrates from which the corresponding solution can be obtained. The difference between the two types of averaging (2.11) and (2.12) is quite small. The averaged contact angle decreases monotonically from the innermost contact line denoted by the index (1) in Fig. 4 towards the outermost contact line denoted by the index (9) in Fig. 4. If we average then the individually averaged cosines over all possible centred solutions we get for the corresponding effective contact angle $\theta^{(b)} = 63.38^\circ$ which differs less than 6% (4.1°) from the theoretical prediction.We take in this averaging all the solutions with equal weight since this is the simplest possible action. In between the nine solutions there is only one (the fourth solution) for which the individually averaged contact angle is very close to the value predicted by the Cassie equation. For the rest of the solutions the Cassie equation does not hold.

It is here the place to make the following comment. In principle it is possible to average the cosine of the contact angle in many different ways: e.g. one can average over all the solutions with equal weights (as we have done); it is possible to take every contact line with weight proportional to the length of the contact line or the weight could be equal to the probability for the realisation of this contact line if there are conditions for different realisations. In particular, in an experiment, it is possible to obtain only certain subset of the solutions due to the experimental setup. More specifically it is possible only to get the two extreme solutions: the one with the smallest radius (maximal averaged contact angle, e.g. $\theta^{(b)}_{\max} = 86.13^\circ$) – solution (1) and the solution (9) with the biggest radius (minimal averaged contact angle – $\theta^{(b)}_{\min} = 41.32^\circ$). Since these angles in this case determine the hysteresis interval $\left[\theta^{(b)}_{\min}, \theta^{(b)}_{\max}\right]$ it is possible to interpret them as the receding and advancing contact angles. In some experimental verifications of the Cassie equation, the Cassie equation is put to test separately for the receding and advancing contact angles which gives its reflection on the interpretation of the final results, e.g. Ref. [2].

For the averaged "projection contact angle" we find the value $\bar{\theta}_{proj} = 57.39^\circ$ which is lower than the value $\theta^{(b)}$=63.38° found numerically by averaging the cosine of the contact angle according to (2.12) and which is even further away from the theoretically predicted by the Cassie equation $\theta^C = 67.5^\circ$

For this kind of substrate (dart board) the assumption for the shape of the contact line made by Li in Ref. [1] generally is not correct. It is possible though to get such type of solution in a very particular case, e.g. if the parameters N_r and e are chosen appropriately. That will mean to choose the distance along the radius in such way that the contact line of the final solution lies entirely between two neighbouring concentric circles and to start

from an initial drop shape whose contact line lies also entirely between the two concentric circles.

5. Summary and conclusion

The wetting properties of model heterogeneous flat substrates were studied numerically in the framework of the classical capillary theory. We obtained the shapes of 3D drops partially wetting such chemically heterogeneous model substrates. We used an iterative minimisation algorithm based on the local variations method. In the considered model dart board substrate it is assumed that the boundaries between the patches with different surface tensions are infinitely sharp ("mesa" defects). A condition for the contact angle was derived when the contact line crosses or pins to such a boundary: either (2.9) or (2.10) holds.

We performed two types of averaging – first an averaging of the cosine of the contact angle along the contact line of the individual drop shape and then over all possible solutions in the considered "ensemble", i.e. all possible centred solutions with constant volume. For every single solution the individual averaging of the contact angle does not satisfy the Cassie equation except one, since the contact line pins at certain parts of the boundaries (which are perpendicular to the radius) separating patches with different surface tensions. However, for the contact angle obtained after averaging over all possible solutions the Cassie equation is reasonably well satisfied – the contact angle differs with less than 6% (4.1°) from the theoretical prediction and is within the error interval of most experimental studies.

This work can be considered as an illustration of some of the ideas of Swain and Lipowsky [8] for statistical averaging on heterogeneous substrates.

Thus we have demonstrated, with this numerical experiment, that to make a conclusion whether Cassie's equation holds, it is very important to analyse the type of the substrate, the shape, the size and the type of heterogeneous patches, as well as the manner in which the equilibrium drop shapes are obtained. It is possible through numerical experiments to model the experimental substrates and to find what would be the observable averaged contact angle and how it depends on the physicochemical properties of the substrate.

REFERENCES

[1] Li, D. Drop Size Dependence of Contact Angles and Line Tensions of Solid-Liquid Systems. *Colloids and Surfaces A: Physicochemical and Eng. Aspects*, **116** (1996), 1–23.

[2] Drelich, J., J. Miller, A. Kumar, G. M. Whitesides. Wetting Characteristics of Liquid Drops at Heterogeneous Surfaces. *Colloids and Surfaces A: Physicochemical and Eng. Aspects*, **93** (1994), 1–13.
[3] Cassie, A. B. D. Contact Angles. *Discuss. Faraday Soc.*, **3** (1948), 11–16.
[4] Laibinis, P., G. M. Whitesides. ω-Terminated Alkanethiolate Monolayers on Surfaces of Copper, Silver, and Gold Have Similar Wettabilities. *J. Am. Chem. Soc.*, **114** (1992), 1990–1995.
[5] Paterson,A., M. Robin, M. Fermigier, P. Jenffer, J. P. Hulin. Effect of Density and Spatial Distribution of Wettability Heterogeneities on Contact Angle. J. *Pet. Sci. En.,* **20** (1998), 127–132.
[6] Woodward, J. T., H. Gwin, D. K. Schwartz. Contact Angles on Surfaces with Mesoscopic Chemical Heterogeneity. *Langmuir*, **16** (2000), 2957–2961.
[7] Joanny, J. F., P. G. de Gennes. A Model for Contact Angle Hysteresis. *J. Chem. Phys.,* **81** (1984), 552–562.
[8] Swain, P., R. Lipowsky. Contact Angles on Heterogeneous Surfaces: A New Look at Cassie's and Wenzel's Laws.*Langmuir*, **14** (1998), 6772–6780.
[9] Decker, E. L., S. Garoff. Using Vibrational Noise To Probe Energy Barriers Producing Contact Angle Hysteresis. *Langmuir,* **12** (1996), 2100–2110.
[10] Decker, E. L., S. Garoff. Contact Line Structure and Dynamics on Surfaces with Contact Angle Hysteresis. *Langmuir,* **13** (1997), 6321–6332.
[11] Adaõ, M. H., de Ruijter, M., Voué, M., J. De Coninck. Droplet Spreading on Heterogeneous Substrates Using Molecular Dynamics. *Phys. Rev. E,* **59** (1999), 746–750.
[12] Urban, D., K. Topolski, J. De Coninck. Wall Tension and Heterogeneous Substrate. *J. Phys. Rev. Lett.*, **76** (1996), 4388–4391.
[13] Collet, P., J. De Coninck, F. Dunlop, A. Regnard. Dynamics of the Contact Line: Contact Angle Hysteresis. *Phys. Rev. Lett.* **79** (1997), 3704–3707.
[14] Andersen, J. V., Y. Brechet. New Macroscopic Hamiltonian for Wetting of a Solid in the Immersion Geometry. *Phys. Rev. Lett.*, **73** (1994), 2087–2090.
[15] Brandon, S., A. Wachs, A. Marmur. Simulated Contact Angle Hysteresis of a Three-Dimensional Drop on a Chemically Heterogeneous Surface: A Numerical Example. *J. Colloid Interface Sci.*, **191** (1997), 110–116.
[16] Brakke, K. The Surface Evolver. *Experimental Mathematics,* **1** (1992), 141–165.
[17] Gibbs, J. W. On the Equilibrium of Heterogeneous Substances. *Trans. Conn. Acad.,* **3** (1876), 108–248; (1878), 343–524.
[18] Wolansky, G., A. Marmur. The Actual Contact Angle on a Heterogeneous Rough Surface in Three Dimensions. *Langmuir,* **14** (1998), 5292–5297.
[19] Iliev, S. D. Iterative Method for the Shape of Static Drops. *Comput. Methods Appl. Mech. Engrg.,* **126** (1995), 251–265.
[20] Chernousko, F. L. Local Variations Method for Numerical Solution of Variational Problems. *J. Comput. Math. and Math. Phys.*, **4** (1965), 749–754 (in Russian).